Enhancement of (nearly) homogeneous fields in a (effective) zero-index cavity

Hai-tao Jiang,[a] Zi-li Wang, Yong Sun, Yun-hui Li, Ye-wen Zhang, Hong-qiang Li, and Hong Chen
Pohl Institute of Solid State Physics, Tongji University, Shanghai, 200092, China and Shanghai Key Laboratory of Special Artificial Microstructure Materials and Technology, Shanghai, 200092, China

(Received 1 February 2011; accepted 5 March 2011; published online 12 April 2011)

Enhanced homogeneous fields are realized in a zero-index medium embedded in Bragg reflectors. When the zero-index medium has Kerr-type nonlinearity, the threshold for optical bistability can be reduced noticeably due to the enhanced uniform fields. Based on a transmission line, we fabricate an effective zero-index medium sandwiched in electric and magnetic walls and experimentally demonstrate the enhanced nearly uniform fields. © *2011 American Institute of Physics*. [doi:10.1063/1.3573506]

I. INTRODUCTION

The threshold of optical bistability depends on the intensity of electric fields inside the nonlinear material. One way to enhance the strength of field inside the nonlinear material is to put it at the center of a one-dimensional (1D) photonic crystal (PC).[1,2] Because of the confinement of two Bragg reflectors, the field is highly localized at the nonlinear material. The thicker the Bragg reflectors are, the stronger the field inside the nonlinear material is. In order to reduce the threshold, we have to use very thick Bragg reflector, which does not facilitate the miniaturization of the device. On the other hand, the field profile in the nonlinear defect is inhomogeneous. The low field parts in the nonlinear material contribute very little to the change of dielectric function, which limits the boost of the nonlinear effect. However, if we increase the whole (inhomogeneous) field, the high field parts may damage the nonlinear material. This poses the question: can we find localized fields in the nonlinear defect to effectively enhance the nonlinear effect, and at the same time limit the damage to the nonlinear material?

Recently, metamaterials with nonpositive permittivity (ε) and/or permeability (μ) have attracted people's interest due to their unique electromagnetic (EM) properties. Besides double-negative metamaterials ($\varepsilon > 0$, $\mu > 0$) (Ref. 3) and single-negative metamaterials including ε-negative (ENG) materials ($\varepsilon < 0$, $\mu > 0$) (Ref. 4) and μ-negative (MNG) materials ($\varepsilon > 0$, $\mu < 0$),[5] zero-index metamaterials (ZIMs) in which $\varepsilon = \mu = 0$ or $\varepsilon = 0$, $\mu \neq 0$ ($\varepsilon \neq 0$, $\mu = 0$) deserve special attention. ZIMs can tailor the radiation phase patterns,[6–8] squeeze EM waves,[9–11] dramatically reduce the reflection (backscattering),[12,13] induce resonant tunneling and enhanced fields,[14,15] or produce additional waves.[16] In 2010, it is found that a ZIM loaded with defects can tune the reflection, realizing either zero or total reflection.[17,18] Based on the Maxwell equations, the fields inside a matched ($\varepsilon = \mu = 0$) ZIM should be homogeneous.[6] In this paper, we put a ZIM inside a cavity surrounded by reflectors. In Sec. II, we find that the homogeneous fields in a ZIM can be greatly amplified due to the confinement of Bragg reflectors. If the dielectric of ZIM has nonlinear part, the enhanced uniform field can boost the nonlinear effect noticeably. Compared to a 1D PC embedded with a nonlinear dielectric, the threshold of bistability in a 1D PC involving a nonlinear ZIM with the same nonlinear coefficient can be reduced to two fifth. In Sec. III, we use a periodic structure consisting of ENG and MNG materials with deep subwavelength thickness as an effective ZIM. Based on transmission line theory, we experimentally demonstrate the enhancement of nearly uniform fields inside an effective ZIM embedded in electric and magnetic walls. Finally, we conclude in Sec. IV.

II. A ZIM CAVITY SURROUNDED BY BRAGG REFLECTORS

Figure 1 is the schematic of a 1D PC embedded with a (nonlinear) medium. In Fig. 1(a) the (nonlinear) medium denoted by *C* is a conventional dielectric while in Fig. 1(b) the (nonlinear) medium denoted by *D* is a ZIM. The dielectric function of the nonlinear medium is

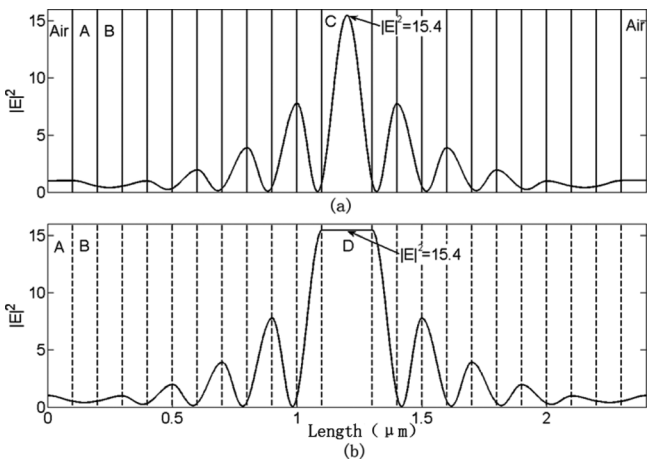

FIG. 1. Schematic of a 1D PC embedded with a dielectric defect denoted by *C* (a) and a ZIM defect denoted by *D* (b), respectively, as well as the corresponding distributions of intensity of electric field. $n_A = n_C = 1.46$, $n_B = 2.13$, $d_A = d_B = 100$ nm, and $d_C = d_D = 200$ nm.

[a]Electronic mail: jiang-haitao@tongji.edu.cn.

$$\varepsilon^{\mathrm{NL}}_{\mathrm{die/ZIM}} = \varepsilon^{L}_{\mathrm{die/ZIM}} + \chi_3 |E|^2, \tag{1}$$

where $|E|^2$ is the intensity of the electric field. In the following calculations, we suppose that $\chi_3 = 0.01$, the linear permittivity of the nonlinear dielectric is $\varepsilon^{L}_{\mathrm{die}} = 1.46^2$. The linear permittivity and permeability of a ZIM are described by a Drude model[18]

$$\varepsilon = \mu = 1 - \frac{\omega_p^2}{\omega(\omega + i\Gamma)}, \tag{2}$$

where $\omega_p = 432.6 \times 2\pi$ THz, $\Gamma = 3.6 \times 10^{-4}\omega_p$, and $\omega = 2\pi f$ is angular frequency. In practice, a nonlinear ZIM can be realized by designing low-loss liquid crystalline-based metamaterials that can possess zero refractive index and a very large Kerr nonlinearity.[19–21] Also, by introducing gain medium into the nanostructured liquid crystal, the loss would be compensated.[22]

The structures in Figs. 1(a) and 1(b) are denoted by $(AB)^5C(BA)^5$ and $(AB)^5ADA(BA)^5$, respectively, where A and B denote SiO_2 and Ta_2O_5 with refractive indices $n_A = 1.46, n_B = 2.13$ (Ref. 23) and thicknesses $d_A = d_B =$ 100 nm, respectively, and 5 is the periodic number. First, we consider the linear case ($\chi_3 = 0$) in which C and D are linear dielectric and ZIM, respectively. The refractive index of C is 1.46. The thickness of dielectric C or ZIM is selected to be 200 nm. At these parameters, the structure in Fig. 1(b) is equivalent to inserting a ZIM at the center of the C layer of the structure in Fig. 1(a). We suppose that light is normally incident on the structure in the z direction and the intensity of the electric field (denoted by $|E|^2$) of the incident wave is 1. Then, in Fig. 2 we use the transfer-matrix method[24] to calculate the transmittances of the structures with (the solid line) and without (the dashed line) ZIM, respectively. It is seen that for both structures a defect mode with the same frequency $f_0 = 432.6$ THz appears. Moreover, the two defect modes almost overlap because inserting a ZIM layer at the center of the C layer does not change the optical length. Though the transmission spectra around f_0 are very near, the field profiles are quite different in two structures. In Fig. 1 we also give the distributions of $|E|^2$ in two structures at $f_0 = 432.6$ THz. It is seen that an inhomogeneous $|E|^2$ is localized in the C layer due to the confinement of Bragg reflectors. One way to further enhance the average $|E|^2$ is increasing the thickness of the Bragg reflectors. However, this method will bring about two problems. One is that the increase of the size of the reflector does not facilitate the miniaturization of device. The other is that the peak value of $|E|^2$ will be very large and damage the nonlinear dielectric. In Fig. 1(a) the peak value of inhomogeneous $|E|^2$ is 15.4. However, in the ZIM layer in Fig. 1(b), $|E|^2$ is homogenous and maintains 15.4 at any place of the ZIM layer. This enhanced uniform field boosts the average $|E|^2$ greatly. Therefore, using a ZIM defect is a good way of enhancing average $|E|^2$ without increasing the size of reflector and the peak value of $|E|^2$ in defect. In the following, we will see the enhanced uniform field can boost the nonlinear effect noticeably.

When χ_3 of a ZIM is considered, we use a nonlinear transfer-matrix method[25] to calculate the intensity of threshold of the structure. We choose three different frequencies of the incident wave, i.e., $f_1 = 429.5$, $f_2 = 427.5$, and $f_3 = 425.5$ THz. Figure 3 shows the variance of intensities of thresholds with these three frequencies. It is seen that, at f_2 or f_3, bistability appears. In Fig. 3, $|E_{\mathrm{up}}|^2$ and $|E_{\mathrm{down}}|^2$ represent the intensity of switch-up and down thresholds for bistability, respectively. At $f_2 = 427.5$ THz, the $|E_{\mathrm{up}}|^2 = |E_{\mathrm{down}}|^2 = 0.66$ which is the critical intensity of threshold and f_2 is the critical frequency of the incident wave. There is no bistability above f_2, e.g., at the frequency of f_1. For comparison, we also calculate the bistability of the structure in Fig. 1(a) when the C layer has the same value of χ_3. In the long-wavelength region of the visible light, the nonlinear dielectric C can be selected to be potassium dihydrogen phosphate[26] whose linear refractive index for extraordinary waves is about 1.46. We find the critical frequency to produce bistability is 426 THz that corresponds to the wavelength of 704 nm and the critical intensity of the threshold is 1.65 that is 2.5 times of the threshold value (0.66) in Fig. 3. In other words, compared to a 1D PC embedded with a nonlinear dielectric, the threshold of bistability in a 1D PC involving a nonlinear ZIM with same χ_3 can be reduced to two fifth.

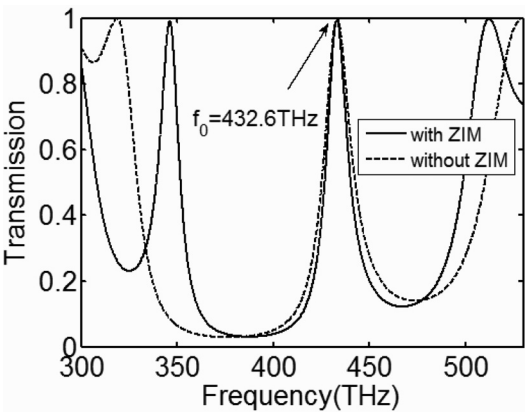

FIG. 2. Transmittances of the structures in Figs. 1(a) and 1(b), respectively. The frequency of the defect mode is $f_0 = 432.6$ THz.

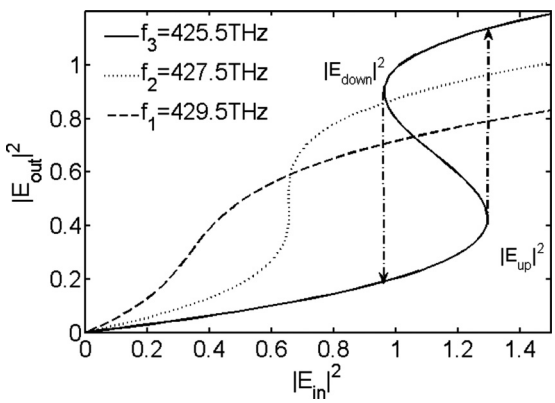

FIG. 3. Output versus input intensity of the structure in Fig. 1(b) for three different frequencies when D layer has Kerr-type nonlinearity.

III. AN EFFECTIVE ZIM CAVITY EMBEDDED IN ELECTRIC AND MAGNETIC WALLS

Here we use ENG and MNG materials with deep subwavelength thickness to construct an effective ZIM. We assume that

$$\varepsilon_1 = \varepsilon_a,\ \mu_1 = \mu_a - \frac{\alpha}{\omega^2}, \tag{3}$$

in MNG materials and

$$\varepsilon_2 = \varepsilon_b - \frac{\beta}{\omega^2},\ \mu_2 = \mu_b, \tag{4}$$

in ENG materials, where α and β are in units of GHz and $\omega = 2\pi f$ is angular frequency. These kinds of dispersion for μ_1 and ε_2 can be realized in a microwave transmission line loaded with lumped capacitors or inductors.[27,28] The thickness of MNG or ENG layer is supposed to be d. The volume averaged permittivity and permeability of a one-dimensional periodic structure composed of ENG and MNG layers can be written as

$$\bar{\varepsilon} = \frac{\varepsilon_1 nd + \varepsilon_2 nd}{2nd} = \frac{\varepsilon_1 + \varepsilon_2}{2},$$
$$\bar{\mu} = \frac{\mu_1 nd + \mu_2 nd}{2nd} = \frac{\mu_1 + \mu_2}{2}, \tag{5}$$

where n is periodic number. At the frequency satisfying $\bar{\varepsilon} = \bar{\mu} = 0$, the wave can tunnel through the structure without any phase delay.[29–31] In general, the fields are localized at each ENG/MNG interface. However, when the value of d is much smaller than the wavelength, the fields can be strongly delocalized and become nearly uniform. In this case, the structure can be taken as an effective ZIM.

Now we use a transmission line loaded with lumped elements to construct an effective ZIM cavity that consists of an electric wall, a magnetic wall, and an effective ZIM. An electric (magnetic) wall only contains ENG (MNG) units denoted by N (M) and an effective ZIM contains ENG/MNG unit cell. We fabricate three types of samples. The first sample hasn't effective ZIM and is denoted by M_6N_6, where 6 is the periodic number. The second and third samples have effective ZIMs with two and six ENG/MNG unit cells, respectively, and they are denoted by $M_6(NM)_2N_6$and $M_6(NM)_6N_6$, respectively. The thickness of each ENG (MNG) unit is 7 mm. Figure 4 is a photograph of the $M_6(NM)_6N_6$ sample fabricated on FR-4 substrate with a thickness of 1.6 mm and relative permittivity of 4.75. The effective MNG (ENG) unit is realized by loading series capacitors (shunt inductors) in the transmission line. The series capacitance and shunt inductance are selected to be $C_i = 4$ pF and $L_i = 10$ nH, respectively. Based on the effective parameter method,[27,28] in the effective MNG unit, $\varepsilon_a = 3.57,\ \mu_a = 1$, and $\alpha = 100.7$, while in the effective ENG unit, $\varepsilon_b = 3.57,\ \mu_b = 1$, and $\beta = 360$. Under these parameters, the frequency satisfying $\bar{\varepsilon} = \bar{\mu} = 0$ is 1.13 GHz. At this frequency, the thickness of the ENG/MNG unit cell (14 mm) is only about one tenth of the wavelength in the substrate. With the aid of CST microwave studio software, we calculate the transmittances of three kinds of samples, as shown in Fig. 5(a). The internal resistance in each lumped element is supposed to be 1 Ω. It is seen that the transmission peaks of all samples occur around 1.12 GHz that is very near to the 1.13 GHz derived from the circuit model. This confirms that the effective ZIM does not introduce additional phase. In Fig. 5(b) we also show the measured transmittances of three samples using Agilent 8722ES Vector Network Analysis. The frequency at the transmission peak of M_6N_6 is 1.1 GHz and that of $M_6(NM)_2N_6$ or $M_6(NM)_6N_6$ is 1.12 GHz that is the same to the simulated one. On the whole, the experiments are in good agreement with the simulations. In Fig. 6 we numerically show the distribution of electric fields in the $x-y$ (horizontal) plane at the middle height of the substrate of $M_6(NM)_6N_6$ at 1.12 GHz. From this top view, one can see that the electric fields are mainly localized at the effective ZIM. In the electric or magnetic wall, the fields are decaying waves. Moreover, the localized fields in the ZIM are almost

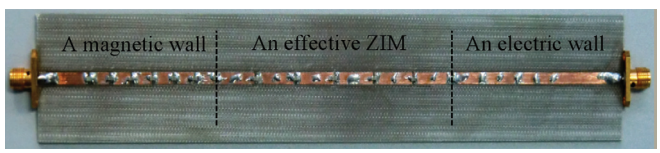

FIG. 4. (Color online) Photograph of $M_6(NM)_6N_6$ fabricated on FR-4 substrate with a thickness of 1.6 mm and relative permittivity of 4.75. The effective ENG (MNG) unit is realized by loading series capacitors (shunt inductors) in the transmission line. $C_i = 4$ pF, $L_i = 10$ nH. An electric (magnetic) wall only contains ENG (MNG) units and an effective ZIM contains ENG/MNG unit cell. The thickness of each ENG (MNG) unit is 7 mm.

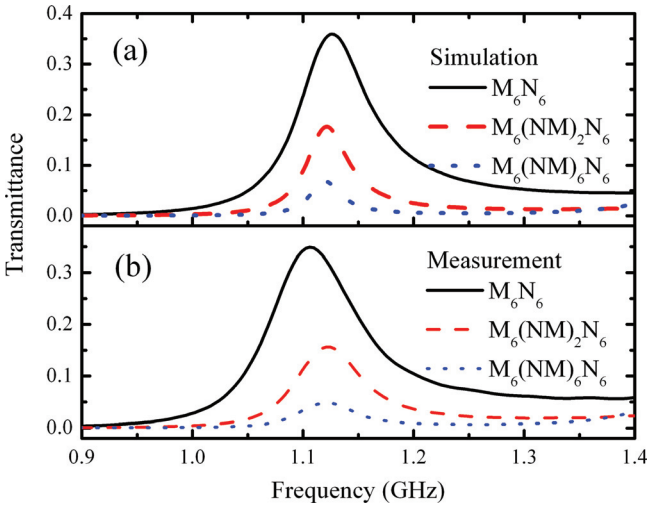

FIG. 5. (Color online) Simulated and measured transmittances of M_6N_6 (the black solid lines), $M_6(NM)_2N_6$ (the red dashed lines), and $M_6(NM)_6N_6$ (the blue dotted lines), respectively.

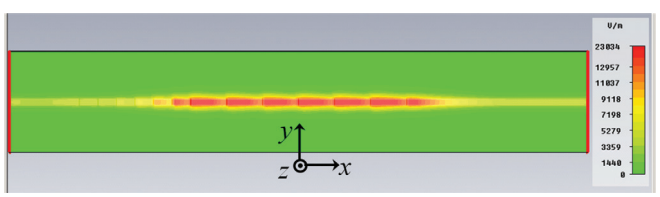

FIG. 6. (Color online) Simulated field distribution in $x-y$ plane at the middle height of the substrate of $M_6(NM)_6N_6$. Boundaries of the effective ZIM are denoted by two dashed lines.

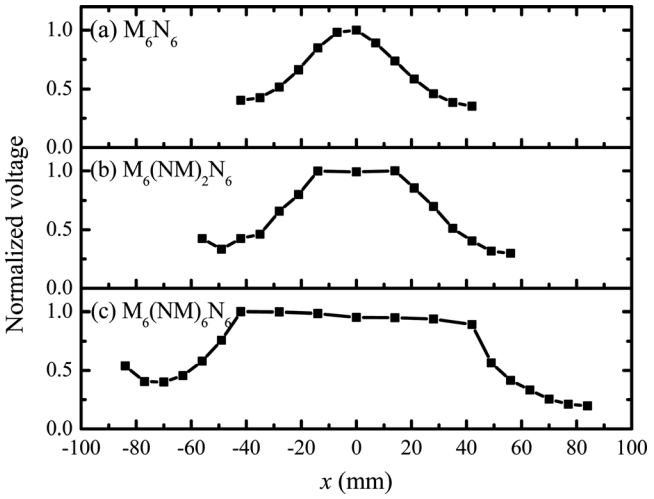

FIG. 7. Measured voltage distributions along the microstrip for (a) M_6N_6, (b) $M_6(NM)_2N_6$, (c) $M_6(NM)_6N_6$, respectively. The symmetric point of the structure is taken as the origin of coordinate.

uniform except that some fields around each metal slit in which a capacitor is inserted are a little bit lower because of scattering. The field patterns in other $x-y$ planes of $M_6(NM)_6N_6$ are similar to that of Fig. 6. In experiment, the fields inside the sample are hardly measured. However, we can measure the voltage between a point of the microstrip and the ground plane. This voltage is the integral of electric field along z direction. After the sine step signals with the frequency corresponding to each transmission peak in Fig. 5(b) are input to the samples, we monitor the voltage signals at the middle point of each ENG (MNG) unit by using a differential probe (Agilent P7260) and an oscilloscope (Tektronix TDS7704B). By analyzing the peak-to-peak value of the recorded dates from the oscilloscope, we obtain the distributions of normalized voltages along the microstrip for three samples, as shown in Fig. 7. The voltage patterns in $M_6(NM)_2N_6$ or $M_6(NM)_6N_6$ [see Fig. 7(b) or 7(c)] clearly show that the voltages in the effective ZIM are enhanced and nearly flat. If nonlinear lumped elements such as varactor diodes[32,33] are loaded in the transmission line, the enhanced uniform voltages will boost the nonlinear effects noticeably. The related work is undergoing.

IV. CONCLUSION

Homogeneous fields in a zero-index medium can be boosted greatly when it is inserted in a cavity. When the zero-index medium has Kerr-type nonlinearity, the threshold for optical bistability can be reduced noticeably due to the enhancement of uniform fields. This enhanced uniform field can make the structure compact and avoid the damage of strong fields to the nonlinear material. Based on transmission line theory, we use two kinds of single-negative materials to construct an effective ZIM cavity and experimentally confirm the enhanced nearly uniform fields.

ACKNOWLEDGMENTS

This work was supported by CNKBRSF (Grant No. 2011CB9220011), by NSFC (Grant Nos. 10634050, 10704055, and 11074187), by the Ph.D. Programs Foundation of SEM (Grant No. 20090072110052), and by the Programs of the Shanghai Science and Technology Committee (Grant Nos. 08dj1400301 and 10ZR1431800).

[1]E. Lidorikis, K. Busch, Q. M. Li, C. T. Chan, and C. M. Soukoulis, Phys. Rev. B **56**(23), 15090 (1997).
[2]N. H. Liu, S. Y. Zhu, and H. Chen, Phys. Rev. B **64**(16), 165105 (2001).
[3]R. A. Shelby, D. Smith, and S. Schultz, Science **292**(5514), 77 (2001).
[4]J. B. Pendry, A. J. Holden, W. J. Stewart, and I. Youngs, Phys. Rev. Lett. **76**(25), 4773 (1996).
[5]J. B. Pendry, A. J. Holden, D. J. Robbins, and W. J. Stewart, IEEE Trans. Microwave Theory Tech. **47**(11), 2075 (1999).
[6]R. W. Ziolkowski, Phys. Rev. E **70**(4), 046608 (2004).
[7]S. Enoch, G. Tayeb, P. Sabouroux, N. GueeČrin, and P. Vincent, Phys. Rev. Lett. **89**(21), 213902 (2002).
[8]A. Alù, M. G. Silveirinha, A. Salandrino, and N. Engheta, Phys. Rev. B **75**(15), 155410 (2007).
[9]M. Silveirinha and N. Engheta, Phys. Rev. Lett. **97**(15), 157403 (2006).
[10]R. P. Liu, Q. Cheng, T. Hand, J. J. Mock, T. J. Cui, S. A. Cummer, and D. R. Smith, Phys. Rev. Lett. **100**(2), 023903 (2008).
[11]B. Edwards, A. Alù, M. E. Young, M. Silveirinha, and N. Engheta, Phys. Rev. Lett. **100**(3), 033903 (2008).
[12]B. Edwards, A. Alù, M. G. Silveirinha, and N. Engheta, J. App. Phys. **105**(4), 044905 (2009).
[13]A. Lakhtakia, Microw. Opt. Technol. Lett. **48**(5), 895 (2006).
[14]K. Halterman and S. M. Feng, Phys. Rev. A **78**(2), 021805 (2008).
[15]N. M. Litchinitser, A. I. Maimistov, I. R. Gabitov, R. Z. Sagdeev, and V. M. Shalaev, Opt. Lett. **33**(20), 2350 (2008).
[16]R. J. Pollard, A. Murphy, W. R. Hendren, P. R. Evans, R. Atkinson, G. A. Wurtz, A.V. Zayats, and Viktor A. Podolskiy, Phys. Rev. Lett. **102**(12), 127405 (2009).
[17]J. M. Hao, W. Yan, and M. Qiu, Appl. Phys. Lett. **96**(10) 101109 (2010).
[18]V. C. Nguyen, L. Chen, and K. Halterman, Phys. Rev. Lett. **105**(23), 233908 (2010).
[19]I. C. Khoo, D. H. Werner, X. Liang, A. Diaz, and B. Weiner, Opt. Lett. **31**(17), 2592 (2006).
[20]D. H. Werner, D. H. Kwon, I. C. Khoo, A. V. Kildishev, and V. M. Shalaev, Opt. Express. **15**(6), 3342 (2007).
[21]I. C. Khoo, A. Diaz, D. H. Kwon, and D. H. Werner, Proc. SPIE **6587**, 658702 (2007).
[22]S. M. Xiao, V. P. Drachev, A. V. Kildishev, X. J. Ni, U. K. Chettiar, H. K. Yuan, and V. M. Shalaev, Nature (London) **466**, 735 (2010).
[23]V. N. Konopsky and E. V. Alieva, Phys. Rev. Lett. **97**(25), 253904 (2006); E. D. Palik, *Handbook of Optical Constants of Solids* (Academic, New York, 1985).
[24]A. Yariv and P. Yeh, *Optical Waves in Crystals* (Wiley, New York, 1984).
[25]J. He and M. Cada, Appl. Phys. Lett. **61**(18), 2150 (1992).
[26]D. N. Nikogosyan, *Nonlinear Optical Crystals: A Complete Survey* (Springer, New York, 2005).
[27]G. V. Eleftheriades, A. K. Iyer, and P. C. Kremer, IEEE Trans. Microwave Theory Tech. **50**(12), 2702 (2002).
[28]A. Sanada, C. Caloz, and T. Itoh, IEEE Microw. Wirel. Compon. Lett. **14**(2), 68 (2004).
[29]A. Alù, and N. Engheta, IEEE Trans. Antenn. Propag. **51**(10), 2558 (2003).
[30]A. Lakhtakia, Int. J. Infrared Millim.Waves **23**(3), 339 (2002).
[31]H. T. Jiang, H. Chen, and S. Y. Zhu, Phys. Rev. E **73**(4), 046601 (2006).
[32]A. B. Kozyrev and D. W. van der Weide, Appl. Phys. Lett. **91**(25), 254111 (2007).
[33]D. A. Powell, I. V. Shadrivov, and Y. S. Kivshar, Appl. Phys. Lett. **94**(8), 084105 (2009).